

**Hepatitis C virus induced degradation of cell death-inducing DFFA-like effector B
leads to hepatic lipid dysregulation**

Emily M Lee¹, Ali Alsagheir², Xianfang Wu^{1,5}, Christy Hammack¹, John McLauchlan³,
Noriyuki Watanabe⁴, Takaji Wakita⁴, Norman M Kneteman², Donna N Douglas², and
Hengli Tang^{1#}

¹Department of Biological Science, Florida State University, Tallahassee, USA;

²Department of Surgery, University of Alberta, Edmonton, Alberta, Canada; ³MRC-

University of Glasgow Centre for Virus Research, Glasgow, UK; ⁴Department of

Virology II, National Institute of Infectious Diseases, Tokyo, Japan.

⁵ Current address: Lab of Virology & Infectious Disease, the Rockefeller University, New
York City, New York USA.

#To whom correspondence should be addressed:

Hengli Tang

Telephone: 850-645-2402; Fax: 850-645-8447; E-mail: tang@bio.fsu.edu.

Running title: HCV-induced CIDEB cleavage

Key words: Lipid droplets, very low density lipoprotein, steatosis, HCV core,
apolipoprotein B.

Word count for abstract: 231; Word count for the text: 4558

ABSTRACT

Chronically infected hepatitis C individuals commonly exhibit hepatic intracellular lipid accumulation, termed steatosis. Hepatitis C virus (HCV) infection perturbs host lipid metabolism through both cellular and viral-induced mechanisms, with the viral core protein playing an important role in steatosis development. We have recently identified a liver protein, the cell death-inducing DFFA-like effector B (CIDEB), as a HCV entry host dependence factor that is downregulated by HCV infection in a cell culture model. Here, we investigate the biological significance and molecular mechanism of this downregulation. HCV infection in a mouse model downregulated CIDEB in the liver tissue, and knockout of CIDEB gene in a hepatoma cell line results in multiple aspects of lipid dysregulation that can contribute to hepatic steatosis, including reduced triglyceride secretion, lower lipidation of very low density lipoproteins, and increased lipid droplet (LD) stability. The potential link between CIDEB downregulation and steatosis is further supported by the requirement of HCV core and its LD localization for CIDEB downregulation, which utilize a proteolytic cleavage event that is independent of the cellular proteasomal degradation of CIDEB.

IMPORTANCE Our data demonstrate that HCV infection of human hepatocytes in vitro and in vivo results in CIDEB downregulation via a proteolytic cleavage event. Reduction of CIDEB protein levels by HCV or gene-editing in turn leads to multiple aspects of lipid dysregulation including LD stabilization. As such, CIDEB downregulation may contribute to HCV-induced hepatic steatosis.

INTRODUCTION

Hepatitis C virus (HCV) is a positive-strand RNA virus and a significant human pathogen. Chronic HCV infection causes liver complications such as steatosis, cirrhosis, and hepatocellular carcinoma. The arrival of new direct-acting antivirals (DAAs) has resulted in markedly improved virologic response in patients with access to these new drugs, but the high cost of the new therapy and the low diagnosis rate of HCV-infected individuals present new challenges for hepatitis C management (1). Furthermore, chronic liver damage can persist even after the infection has been cleared, so HCV pathogenesis remains an area of research highly significant for human health.

The HCV life cycle and pathogenesis are intimately linked to host lipid metabolism (2). On one hand, lipids are involved in multiple stages of the infection cycle. HCV virions are assembled on lipid droplets (LDs) (3) and associated with host lipoproteins to form lipo-viral-particles (LVP) for infection (4); the productive entry of HCV is aided by several molecules involved in lipid uptake (5-7); replication of HCV genome critically depends on a lipid kinase (8, 9) and is regulated by lipid peroxidation (10). On the other hand, HCV infection profoundly disturbs lipid metabolism pathways (11). HCV patients exhibit enhanced lipogenesis (12), consistent with in vitro results showing that HCV infection upregulates genes encoding sterol regulatory element binding protein-1c (SREBP-1c) and fatty acid synthase (FASN), both important for the intracellular lipid synthesis pathway (13-16). More recently, the 3'-UTR of HCV was shown to, upon binding of DDX3, activate I κ B kinase- α and trigger biogenesis of LDs (17). Consequently, liver

steatosis, the intracellular accumulation of lipids, is a common histological feature of chronic hepatitis C patients, especially in those with genotype 3 infection (18, 19). The mechanisms of viral-induced steatosis may involve both increased lipogenesis and reduced lipolysis and secretion (20, 21). The expression of HCV core protein was shown to recapitulate HCV-induced steatosis in a transgenic mouse model (22, 23) and the localization of core protein to LDs may be important for intracellular LD accumulation and steatosis induction (24-26).

The cell death-inducing DFFA-like effector (CIDE) family proteins, CIDEA, CIDEB and CIDEC/ fat-specific protein 27 (Fsp27), were originally identified using a bioinformatics approach based on their homology to the N-terminal domain of DNA fragmentation factors (27). While CIDEA and CIDEC are more widely expressed, CIDEB is mostly expressed in liver cells (27) and induced during hepatic differentiation of stem cells (28, 29). Although these proteins can induce cell death when overexpressed (27, 30, 31), gene knockout (KO) experiments in mice indicate that their function relates mostly to lipid metabolism in vivo (32-34). A role of CIDEB in very-low-density lipoprotein (VLDL) lipidation, VLDL transport, and cholesterol metabolism has been reported in non-primate cell culture models (34-36). We previously characterized a role of CIDEB in a late step of HCV entry into hepatocytes (29). In this study, we investigate the molecular mechanism and biological consequence of HCV-induced downregulation of CIDEB. We demonstrate that CIDEB protein is normally regulated through the ubiquitin-mediated proteasome pathway and that HCV infection further downregulates CIDEB by inducing CIDEB protein degradation, most likely through proteolytic cleavage. This HCV-

mediated degradation of CIDEB requires the expression of HCV core, and downregulation of CIDEB protein was observed in a HCV-infected humanized mouse model. In addition, we demonstrate that gene knockout of CIDEB in a human hepatoma cell line reduces the secretion of triglycerides (TGs) and stabilizes cytoplasmic LDs in a manner similar to HCV infection. Core-dependent CIDEB downregulation in vivo may contribute to hepatic steatosis in the setting of HCV infection.

MATERIALS AND METHODS

Antibodies, compounds, and inhibitors. The following antibodies and chemicals were used in this study: anti-JFH-1 core and NS3 (BioFront Technologies Inc., FL); anti-CIDEB, GAPDH, Ku80 (Santa Cruz Biotechnology, TX); anti-DENV-NS3 (Genetex, CA); FITC and TRITC conjugated anti-rabbit and anti-mouse IgGs (Sigma Aldrich, MO); oleic acid (OA), Oil Red O (ORO), cyclohexamide (CHX), Triacsin C (TriC), PF-429242 (Sigma Aldrich, MO); and MG132 (EMD-Millipore, MA).

Cell culture and HCVcc Infection. Huh-7.5 cells were provided by Dr. Charles Rice (Rockefeller University) and Apath LLC (NY). Generation of the CIDEB knockdown and knockout cell lines have been previously described (29). FLAG-CIDEB stable cells were generated using a human immunodeficiency virus (HIV)-based lentiviral vector expressing FLAG-CIDEB cDNA. Briefly, we transduced Huh-7.5 CIDEB KO cells with pHIV-7-IRES-FLAG-CIDEB, selected stable populations with 1.2µg/mL puromycin for three weeks then obtained single cell clones. For genotype 2 HCVcc infection, cells were inoculated with either wild type JFH-1 or several high titer variants: JFH-1/Ad16

(provided by Dr. Guangxiang Luo, University of Alabama at Birmingham), Mut4-6, and JLSO-III (37, 38) for 6-8 hours at 37°C, followed by three PBS washes before being changed into fresh media. The cell lines harboring infection by genotype 3 viruses have been described previously (39).

Infection with other viruses. Huh-7.5 cells were seeded onto glass cover slips in 12-well plates and infected for 16 hours with VSV-GFP (kindly provided by Dr. Fanxiu Zhu, Florida State University) or DENV for 48 hours.

Plasmid construction and mutagenesis. The HA-ubiquitin plasmid was a gift from Dr. Fanxiu Zhu (Florida State University). For generation of the K173A CIDEB construct, mutagenesis was performed using the QuikChange Site-Directed Mutagenesis Kit (Agilent Technologies, CA) according to manufacturer's instructions.

Immunofluorescence Analysis. Cells seeded on slides were fixed in 4% paraformaldehyde for 10 minutes, followed by three 10-minute washes in phosphate buffered saline (PBS) at room temperature and blocked in PBTG (PBS containing 0.1% Triton X-100, 10% normal goat serum, and 1% BSA) at room temperature for 2 hours. Slides were then incubated with primary antibody at either room temperature for 1 hour or at 4° C for overnight. Following primary antibody incubation, slides were washed with PBS for three subsequent 15-minute washes, and then incubated with secondary antibody for 1 hour at room temperature, followed by three subsequent 15-minute washes with PBS. Slides were mounted and nuclei stained using VECTASHIELD

(Vector Labs, CA). Oil Red O (ORO) staining was carried out according to supplier instructions.

Western blot. Cells were harvested by trypsinization, pelleting, and subsequent lysis in 1X Laemmli buffer and boiled, or directly lysed in 1x Laemmli buffer and boiled.

Electroporation of viral RNA. In vitro transcription and electroporation of HCV RNAs were performed as previously described (29). Viral J6/JFH-1/Gluc and deletion mutants (Δ E1/E2, Δ core, GNN) RNA were generated in vitro using a MEGAscript T7 kit (Ambion, TX) and purified by phenol-chloroform extraction. For electroporation, 10ug of RNA was used for 4×10^6 cells in a volume of 400ul low serum media in a 4mm cuvette (VWR) using the Gene Pulser Xcell Electroporation System (Bio-Rad, CA). Medium was changed four hours post-electroporation. Samples were collected at four hours post electroporation to control for electroporation efficiency. Samples were collected either by direct lysis with 1x Laemmli buffer and boiled, or by incubation with trypsin, followed by pelleting and lysis by boiling in 1x Laemmli buffer for Western blot analysis. The Jc1/GLuc constructs were provided by Dr. Brett Lindenbach (Yale University).

Cell Viability Assay. Huh-7.5 cells were seeded into 96-well plates before treatment with indicated compound for 24 hours. Cells were then assayed in biological triplicate using the CellTiter-Glo Luminescent cell viability kit according to manufacturer instructions (Promega, WI).

Co-Immunoprecipitation. Huh-7.5 cells were co-transfected with FLAG-CIDEB or HA-ubiquitin constructs. 18-24 hours after transfection, cells were treated with 10 μ M MG132, then washed three times with ice-cold PBS and solubilized with lysis buffer (50 mM Tris/HCl, pH 7.5, 150 mM NaCl, 1.0 % NP-40, 5 mM EDTA, 5 mM EGTA, 15 mM MgCl₂, 60 mM β -glycerophosphate, 0.1 mM sodium orthovanadate, 0.1 mM NaF, 1 mM PMSF, 1 \times proteinase inhibitor cocktail) for 5 minutes on ice, and then rotated for 1 hour at 4°C. Cell lysate was centrifuged at 12,000 x g for 10 minutes at 4°C to remove any insoluble material, and then subjected to IP with EZview anti-Flag M2 or anti-HA affinity beads (Sigma-Aldrich, MO) according to manufacturer's instructions. The beads were collected by centrifugation and then washed gently three times with lysis buffer supplemented with protease inhibitors. Beads and bound protein were boiled in 2 \times Laemmli buffer and analyzed via Western blot.

CIDEB stability assays. To analyze stability of endogenous CIDEB, Huh-7.5 cells were treated with 2.5 μ g/mL CHX for the indicated amounts of time before being directly boiled in 1 \times Laemmli buffer and analyzed via western blot. For CIDEB mutants, cells were transfected with the mutant constructs for 18 hours, treated with 2.5 μ g/mL CHX for 4 hours and analyzed similarly. For proteasome inhibition, cells were treated with 10 μ M MG132 for 18 hours. For lipid loading, cells were electroporated with JFH-1 or infected with JFH-1/AD16 for 24 hours and then incubated in media containing 0 μ M, 100 μ M, or 400 μ M OA, for 20 hours before western blot analysis.

Lipid droplet purification. Huh-7.5 cells were infected with JFH-1/AD16 for 42 hours and then treated with 375uM OA for 14 hours. Cells were harvested in ice cold PBS and stored at -80. Cell pellets were fractionated following a modified previously published protocol (40). Briefly, cell pellets were dounce homogenized in buffer A (20mM tricine, 250mM sucrose, 1mM PMSF, pH 7.8), overlayed with buffer B (20mM HEPES, 100mM KCl, 2mM MgCl₂, pH 7.4) and ultracentrifuged at 270,000 x g for 1 hour. The floating crude LD fraction was collected and then centrifuged at 14,000 x g for 10 minutes and residual underlying liquid and pellet removed. Total LD was then washed with buffer B four times. Lipids were dissolved with equal amounts chloroform and acetone, and the resulting protein pellet was resuspended in 1x laemmli buffer. Total protein amount was measured using the Bio-Rad DC protein assay. For western blot analysis, 15ug of whole cell lysate and 7.5ug of purified LD proteins were used.

Lipid droplet stability analysis. Naïve and 60 hour post-JFH-1/AD16 infected Huh-7.5 or naïve Huh-7.5-CIDEB KO cells (single-cell clones #03 and #11) were seeded at low confluence (10%) onto coverslips in 12-well plates and treated with 375μM OA for 14-20 hours. The cells were then washed three times with PBS, further incubated in fresh, OA-free containing 5.5μM TriC or 40μM PF-429242 for 24 hours before LDs were visualized using ORO staining.

VLDL Density Analysis. Naïve and 60 hour post-JFH-1/AD16 infected Huh-7.5 or naïve Huh-7.5/CIDEB-KO clone #11 cells were incubated in a lipid-rich medium (DMEM containing 375μM OA, 10% FBS, and non-essential amino acids) for 14 hours, washed

three times with PBS, then changed into DMEM for 8 hours. Collected supernatant was fractionated into 11 fractions using a continuous 10-40% iodixanol gradient (77,160 x g for 17 hours at 4°C). The fractions were analyzed for ApoB content using an ApoB100 detection kit (Mabtech, OH).

Triglyceride storage and secretion. Huh-7.5 or Huh-7.5/CIDEB-KO clone #11 cells were incubated in the lipid-rich media for 20 hours, washed three times with PBS, then incubated in DMEM and collected by scraping in ice-cold PBS and lysed via sonication. Cell lysate and supernatant were analyzed for TG content using a TG detection kit (Sigma Aldrich, MO).

Humanized mouse model sample collection. These methods have been described previously (41).

RESULTS

HCV infection downregulates CIDEB in vitro and in vivo. We have previously observed that JFH-1/HCVcc infection resulted in a lower CIDEB protein level on western blots without reducing CIDEB mRNA in cultured cells (29). To facilitate single-cell, immunofluorescence-based detection of CIDEB, we generated a stable FLAG-CIDEB-expressing Huh-7.5-based cell line (FLAG-CIDEB CBKO#3) that lacked endogenous CIDEB expression. Indeed, infection of this cell line and subsequent dual-staining of HCV-infected cells for HCV NS3 and CIDEB revealed a pattern of mutual exclusivity between HCV expression and CIDEB protein (Fig. 1A, top panel), consistent

with a HCV-mediated CIDEB downregulation. The uninfected cells exhibited a more uniform expression pattern of CIDEB (Fig. 1A, second panel) and VSV or Dengue virus infection of the FLAG-CIDEB CBKO#3 cells did not result in this pattern of exclusion between infection and CIDEB protein (Fig. 1A, bottom panels). Western blotting confirmed the downregulation of CIDEB protein by JFH-1, a genotype 2 virus, and its derivatives (Fig. 1B). We also tested a genotype 3 virus (39), for CIDEB downregulation. Infection of Huh-7.5.1 cells, a derivative of the Huh-7.5 cell line, with three different clones of a GT3a virus resulted in virus production with different efficiencies. Higher levels of core protein (as measured by ELISA) were correlated with a reduction of endogenous intracellular CIDEB protein level, similar to what was observed in the JFH-1-infected cells (Fig. 1B). The less pronounced downregulation of CIDEB protein by these GT3 viruses is a likely result of lower infection efficiencies of these isolates, rather than a genotype specific effect on CIDEB degradation (Fig. 1B). Finally, we investigated if endogenous human CIDEB is downregulated by HCV infection in vivo. We analyzed liver samples of human-liver SCID/uPA mice with or without infection by a genotype 1a HCV derived from human serum (41). As shown in Fig. 1C, liver tissues from HCV infected mice expressed lower overall CIDEB proteins than those from similarly transplanted but uninfected animals. Together, these results suggest that CIDEB downregulation by HCV infection occurs with multiple genotypes and within the liver environment.

CIDEB is normally regulated at the cellular level by ubiquitin-mediated

proteasomal degradation. In addition to HCV infection, the expression level of CIDEB

in liver cells is also regulated by a variety of stimuli (29, 42). In order to understand

whether HCV enhances normal cellular degradation of CIDEB or utilizes a separate,

distinct mechanism, we investigated the cellular mechanism of CIDEB regulation in

uninfected hepatocytes. We performed CHX inhibition experiments to determine the

half-life of the CIDEB protein in uninfected cells. As shown in Fig. 2A, CIDEB is a short-

lived protein with an estimated half-life of < 60 minutes, which is near the low end

spectrum of mammalian protein half-lives and well below the average protein turnover

rate (10-20 hours) in human cells reported previously (43). The GAPDH protein was

used as a loading control because it has been reported to have a long half-life of 40-50

hours and thus unlikely to change for the duration of the experiments performed here

(44). To determine whether the rapid turnover of CIDEB is mediated by proteasomes,

we treated the cells with MG132, a proteasome inhibitor, and determined CIDEB protein

level with immunoblotting. An increase of CIDEB level was observed with MG132

treatment in both Huh-7.5 cells and a derivative cell line that harbored a small-hairpin

RNA (shRNA) against the CIDEB mRNA (Fig. 2B), suggesting that proteasomes play a

role in regulating CIDEB protein stability. Because canonical proteasome targeting is

mediated by poly-ubiquitylation of the target protein, we tested whether inhibition of

proteasome-mediated protein degradation results in accumulation of poly-ubiquitinated

CIDEB. Treatment of cells co-transfected with FLAG-CIDEB and HA-ubiquitin with

MG132 resulted in accumulation of poly-ubiquitylated CIDEB, (Fig. 2C), indicating that

the CIDEB protein level is regulated by ubiquitylation and the proteasome. Ubiquitins

are commonly linked to lysine residues on target proteins. To identify the lysine residue(s) responsible for CIDEB ubiquitylation, we generated truncation mutants of CIDEB cDNA where regions containing specific lysine residues were removed (Fig. 2D). The deletion of amino acids 166 through 195, which contained the two lysine residues, K172 and K173, significantly stabilized the protein (Fig. 2E). Site-directed mutagenesis further confirmed that lysine 173 (K173) is important for CIDEB degradation because its replacement by an alanine residue stabilized the protein (Fig. 2F).

HCV infection triggers a proteolytic cleavage of CIDEB in a core-dependent manner. Consistent with our previous report (29), immunoblot analysis of HCVcc infected Huh-7.5 cells showed reduced CIDEB levels compared to uninfected Huh-7.5 cells. Interestingly, in experiments where the samples were directly lysed in protein loading buffer and where protein degradation was minimized after cell lysis, the reduction of CIDEB full-length protein coincided with the appearance of a faster-migrating species that is recognized by the anti-CIDEB antibody (Fig. 3A). This species was not observed when immunoblot analysis was performed with an IgG control instead of anti-CIDEB (not shown), indicating that this faster migrating species is a CIDEB cleavage product and that HCV infection may trigger proteolytic cleavage of CIDEB. MG132 treatment did not reduce the HCV-activated proteolytic cleavage of CIDEB (Fig. 3B), indicating that the cellular and viral-induced CIDEB downregulation use distinct mechanisms. A similar band was also observed in the aforementioned FLAG-CIDEB CBKO#3 cells infected with HCVcc that was detectable by anti-CIDEB antibody (Fig. 3C) but not by anti-FLAG antibody. Note that the FLAG epitope was fused to the N-terminus

of CIDEB, which is unstable upon cleavage and cannot be detected with the anti-FLAG antibody either in IFA (Fig. 1A) or on western blots (data not shown). To identify viral determinants involved in CIDEB downregulation and cleavage, immunoblot analysis of CIDEB was performed following electroporation of cells with one of three different mutant HCV genomes: one with an internal in-frame deletion in the HCV core gene (Δ core), one with mutations in the active site of the viral polymerase (GNN), and one with the deletion of the E1E2 genes (Δ E1/E2). While the wildtype genome efficiently downregulated CIDEB full-length protein and resulted in the appearance of the cleavage product (Fig. 3D), the Δ core mutant failed to reduce CIDEB level or trigger cleavage despite expressing similar amounts of the HCV NS3 protease (Fig. 3D). The polymerase-deficient mutant GNN failed to replicate and did not express detectable amounts of HCV proteins. It also failed to downregulate CIDEB as expected (Fig. 3D). On the other hand, the Δ E1/E2 mutant was still able to downregulate CIDEB and to activate cleavage (Fig. 3E). These results demonstrate that the HCV core, but not the glycoproteins, is required for CIDEB downregulation via a mechanism independent of the HCV protease.

Role of LDs and core's LD localization in CIDEB downregulation. HCV core localizes to the surface of LDs in HCV infected cells, which may result in a competition with other LD-localized proteins such as CIDEB. To address this possibility, we investigated whether the amount of intracellular lipids and LDs affect CIDEB protein stability. First, we inhibited LD formation in Huh-7.5 cells using lipid inhibitors and then determined whether CIDEB level was reduced. Two structurally distinct inhibitors were

321 used. 4-[(Diethylamino)methyl]-N-[2-(2-methoxyphenyl)ethyl]-N-(3R)-3-
322 pyrrolidinylbenzamide (PF-429242) is a reversible inhibitor of cholesterol and fatty acid
323 synthesis, acting by blocking SREBP cleavage; Triacsin C (TriC) is an inhibitor of long-
324 chain fatty acid acyl-CoA synthetase. Both compounds inhibited LD formation as
325 expected without significantly affecting cell viability (Fig. 4A and 4B), and more
326 importantly, they also effectively reduced CIDEB protein in Huh-7.5 cells (Fig. 4C and
327 4D). The reduction of CIDEB protein was not due to a decrease in CIDEB mRNA level
328 upon treatment (Fig. 4E), and we did not detect the putative cleavage product (data not
329 shown) in these experiments. In the second line of experiments, we augmented
330 intracellular LD formation by feeding the cells with excess oleic acid (OA) and then
331 determined if this lipid loading, which significantly increased the number of LDs in Huh-
332 7.5 cells (Fig. 4F), could modulate CIDEB level in HCV-infected cells. Loading the cells
333 with OA restored the CIDEB protein level in HCV-infected cells to a similar level of that
334 in uninfected, unloaded cells (Fig. 4G), consistent with the hypothesis that increased LD
335 availability can counteract the effect of HCV infection on CIDEB level. To directly
336 address if the localization of HCV core protein to LDs is required for CIDEB
337 downregulation, we took advantage of a core double proline mutant that reduced its LD
338 association without significantly affecting its expression level (45). Electroporation of the
339 full-length HCV genome containing these core mutations (JFH_{DP}) was still capable of
340 activating the pathway that leads to CIDEB cleavage, but the extent of downregulation
341 was reduced compared to the wildtype (Fig. 5A). The NS3 expression levels were
342 comparable, suggesting that core protein and its association with LDs, but not overall
343 viral protein expression, is correlated with CIDEB downregulation. In addition, the

reduction of CIDEB protein upon HCV infection was even more pronounced in the LD fractions (Fig. 5B). Localization of both CIDEB and core onto the surface of the same LDs could also be detected when we co-expressed these proteins to a level in uninfected cells (Fig. 5C).

CIDEB knockout stabilizes LDs in the presence of excess lipids. A mechanism by which HCV core may contribute to hepatic steatosis is through the stabilization of cytoplasmic LDs (25, 26). Consistent with these reports, we also observed increased LD stability in hepatoma cells infected with HCV as compared to non-infected (Fig. 6A). We determined if suppression of CIDEB could similarly affect LD stability. We recently generated Huh-7.5 cell clones that have the CIDEB gene knocked out using TALEN-based genome editing (29). In the absence of lipid loading, both the CIDEB shRNA and the CIDEB KO reduced the number of LDs (29). When the cells were fed with lipid-rich medium that contained oleic acid, however, both parental and KO cells were able to form LDs (Fig. 6B). To determine if CIDEB KO affects LD stability, we used TriC to block the synthesis of fatty acids after lipid loading. Under these conditions, the KO cells contained many more large LDs than the wildtype cells did (Fig. 6C), likely due to the reduced secretion of the VLDL/LDLs, which can slow down the depletion of their intracellular reservoir (the cytoplasmic LDs) in the absence of new lipid synthesis.

CIDEB-knockout in vitro phenocopies the alteration of lipid profiles caused by HCV infection. Given the involvement of CIDE family proteins in lipid metabolism, we determined the effect of CIDEB deficiency on the VLDL secretion and intracellular TG

levels in a human hepatoma cell line. It has previously been shown that Huh-7.5 cells secrete very little amounts of TG; however, these cells can be used for VLDL studies if supplemented with exogenous OA in order to first expand the intracellular TG pool (21). Therefore, we supplied cells with exogenous OA prior to measuring TG secretion. Compared with wildtype Huh-7.5 cells, the CIDEB KO cells had a reduced level of TG secretion accompanied by a slight increase of intracellular TG level after lipid loading (Fig. 7A). In addition, the CIDEB KO cells secreted less ApoB-containing VLDLs (Fig. 7B). Analysis of secreted ApoB particles revealed an overall increase of density of the ApoB particles secreted from the CIDEB KO cells (Fig. 7C), suggesting a reduction in intracellular lipidation of ApoB. Overall, the VLDL density profile of ApoB particles secreted from CIDEB KO cells is similar to the density profiles for ApoB secreted from HCV infected cells (Fig. 7D) and differs from wildtype, uninfected cells.

Discussion

In this study, we demonstrate that HCV infection reduces full-length CIDEB protein by activating a proteolytic cleavage event. This downregulation was independent of HCV glycoproteins but requires HCV core and may play a role in HCV-induced lipid accumulation in HCV pathogenesis.

HCV-induced modulation of CIDEB protein is distinct from the normal ubiquitin-proteasomal regulation of the protein, which has also been shown to modulate CIDEA

and CIDEC proteins in other cell types (46, 47). The fine-tuning of CIDE family proteins by proteasomes may be critical for maintaining normal cell physiology. On one hand, the CIDE proteins readily induced cell death in a variety of cell types when overexpressed (27, 30, 31); on the other hand, suboptimal levels of CIDEB can lead to an imbalance of lipid metabolism. Notably, apoptosis induction likely accounts for a reported antiviral effect of CIDEB overexpression in cell culture (48), where the authors concluded that CIDEB's ability to reduce HCV RNA levels in replicon cells was correlated with its pro-apoptotic function.

A specific cleavage in response to a stimulus such as viral infection has not been reported for any CIDE proteins but appears to be the mechanism of HCV-mediated downregulation of CIDEB. Previous studies have shown CIDEB KO mice exhibit increased resistance to diet-induced steatosis and reduced lipogenesis (34). Similarly, we have observed LD formation being impaired in uninfected human hepatoma cells when CIDEB expression is reduced by shRNA or eliminated by gene knockout (29). Upon HCV infection which increases lipogenesis (12, 14, 23), however, CIDEB depletion causes altered VLDL profiles and leads to intracellular lipid accumulation. Similarly, when cells were fed with excess lipids, suppression of CIDEB stabilized cytoplasmic LDs. The observation that genetic ablation led to perturbations of the lipid secretion pathway similar to those caused by HCV infection suggest a connection between CIDEB modulation and lipid regulation in infected cells. Consistent with this hypothesis, HCV-induced CIDEB downregulation was observed in cultured cells infected with a genotype 3 virus as well as in infected liver tissues of a HCV mouse

model. The in vivo data is consistent with a previous report showing that transgenic expression of HCV proteins in mice led to a reduction of CIDEB protein (31), even though the cleavage product was not detectable from the in vivo samples, which could be due to the labile nature of the protein, especially considering the fixing and processing necessary for the live tissues. Combined with a growing body of evidence supporting the function of the CIDE proteins in lipid regulation and the reported role of HCV core in virus-induced steatosis, our results support a model (Fig. 8) where chronic HCV infection of human hepatocytes results in sustained reduction of CIDEB protein, which in turn contributes to hepatic lipid dysregulation and steatosis.

Localization of HCV core to the surface of LDs is important for HCV assembly (3), and colocalization of a LD-targeted cellular factor, TIP47, with NS5A and core on LDs may be required for HCV replication and release (49). On the other hand, the extensive coating of the LD surface by HCV core protein in the infected hepatocytes can lead to displacement of native LD proteins such as CIDEB and perilipins. Such a competition has been shown to play a role in the downregulation of perilipin 2 (PLIN2) protein, also known as adipocyte differentiation-related protein (ADRP). The dissociation of ADRP protein from LDs, as a result of core competition, led to reduced stability of ADRP (50), presumably due to increased exposure to protease(s). Our results suggest a role of HCV core's LD localization in CIDEB downregulation, consistent with such a competition/displacement model that is distinct from HCV NS3/4A-mediated cleavage of critical antiviral signaling proteins (51, 52). Of note, no specific interaction between CIDEB and HCV core was detected in co-IP experiments (data not shown).

436

437 The displacement of CIDEB from the LD surface may expose the protein to a protease
438 that normally does not have access to CIDEB. Alternatively, the presence of HCV core
439 during infection may activate a protease that can cleave CIDEB. Preliminary
440 experiments testing different classes of protease inhibitors, including Calpain and
441 caspase inhibitors, yielded inconclusive results so far. The Δ core mutant genome
442 expresses both NS2 and the NS3/4A proteases encoded by HCV but failed to
443 downregulate CIDEB protein or trigger the proteolytic cleavage, suggesting the
444 involvement of cellular, rather than viral proteases. The identification of the specific
445 protease(s) that is responsible for cleaving CIDEB in a HCV-dependent manner can
446 provide promising candidates for targeted interventions of lipid dysregulation.

447

448 Funding source:

449 This work was supported by NIH/NIAID R56 AI107763 (HT), R21 AI111250 (HT), and
450 CIHR grant 52973 (NMK, DND). EML is supported by a pre-doctoral fellowship from the
451 American Heart Association. NMK is also supported by the Capital Health Chair in
452 Transplantation Research from Alberta Health Services, Canada.

453

454 **ACKNOWLEDGMENTS**

455

456 We would like to thank the following colleagues for providing reagents: Guangxiang G.
457 Luo; Charles M. Rice; Fanxiu Zhu; Brett Lindenbach. We thank Stephen Frausto,
458 Christopher Pu, and Jaime Lewis for technical assistance.

References

1. **Pawlotsky JM.** 2013. Treatment of chronic hepatitis C: current and future. *Curr Top Microbiol Immunol* **369**:321-342.
2. **Schaefer EA, Chung RT.** 2013. HCV and host lipids: an intimate connection. *Semin Liver Dis* **33**:358-368.
3. **Miyanari Y, Atsuzawa K, Usuda N, Watashi K, Hishiki T, Zayas M, Bartenschlager R, Wakita T, Hijikata M, Shimotohno K.** 2007. The lipid droplet is an important organelle for hepatitis C virus production. *Nat Cell Biol* **9**:1089-1097.
4. **Lindenbach BD, Rice CM.** 2013. The ins and outs of hepatitis C virus entry and assembly. *Nat Rev Microbiol* **11**:688-700.
5. **Monazahian M, Bohme I, Bonk S, Koch A, Scholz C, Grethe S, Thomssen R.** 1999. Low density lipoprotein receptor as a candidate receptor for hepatitis C virus. *J Med Virol* **57**:223-229.
6. **Scarselli E, Ansuini H, Cerino R, Roccasecca RM, Acali S, Filocamo G, Traboni C, Nicosia A, Cortese R, Vitelli A.** 2002. The human scavenger receptor class B type I is a novel candidate receptor for the hepatitis C virus. *EMBO J* **21**:5017-5025.
7. **Sainz B, Jr., Barretto N, Martin DN, Hiraga N, Imamura M, Hussain S, Marsh KA, Yu X, Chayama K, Alrefai WA, Uprichard SL.** 2012. Identification of the Niemann-Pick C1-like 1 cholesterol absorption receptor as a new hepatitis C virus entry factor. *Nat Med* **18**:281-285.
8. **Berger KL, Cooper JD, Heaton NS, Yoon R, Oakland TE, Jordan TX, Mateu G, Grakoui A, Randall G.** 2009. Roles for endocytic trafficking and phosphatidylinositol 4-kinase III alpha in hepatitis C virus replication. *Proc Natl Acad Sci U S A* **106**:7577-7582.
9. **Tai AW, Benita Y, Peng LF, Kim SS, Sakamoto N, Xavier RJ, Chung RT.** 2009. A functional genomic screen identifies cellular cofactors of hepatitis C virus replication. *Cell Host Microbe* **5**:298-307.
10. **Yamane D, McGivern DR, Wauthier E, Yi M, Madden VJ, Welsch C, Antes I, Wen Y, Chugh PE, McGee CE, Widman DG, Misumi I, Bandyopadhyay S, Kim S, Shimakami T, Oikawa T, Whitmire JK, Heise MT, Dittmer DP, Kao CC, Pitson SM, Merrill AH, Jr., Reid LM, Lemon SM.** 2014. Regulation of the hepatitis C virus RNA replicase by endogenous lipid peroxidation. *Nat Med* **20**:927-935.
11. **Diamond DL, Syder AJ, Jacobs JM, Sorensen CM, Walters KA, Proll SC, McDermott JE, Gritsenko MA, Zhang Q, Zhao R, Metz TO, Camp DG, 2nd, Waters KM, Smith RD, Rice CM, Katze MG.** 2010. Temporal proteome and lipidome profiles reveal hepatitis C virus-associated reprogramming of hepatocellular metabolism and bioenergetics. *PLoS Pathog* **6**:e1000719.
12. **Lambert JE, Bain VG, Ryan EA, Thomson AB, Clandinin MT.** 2013. Elevated lipogenesis and diminished cholesterol synthesis in patients with hepatitis C viral infection compared to healthy humans. *Hepatology* **57**:1697-1704.
13. **Waris G, Felmlee DJ, Negro F, Siddiqui A.** 2007. Hepatitis C virus induces proteolytic cleavage of sterol regulatory element binding proteins and stimulates their phosphorylation via oxidative stress. *J Virol* **81**:8122-8130.
14. **Yang W, Hood BL, Chadwick SL, Liu S, Watkins SC, Luo G, Conrads TP, Wang T.** 2008. Fatty acid synthase is up-regulated during hepatitis C virus infection and regulates hepatitis C virus entry and production. *Hepatology* **48**:1396-1403.

15. **Fujino T, Nakamuta M, Yada R, Aoyagi Y, Yasutake K, Kohjima M, Fukuizumi K, Yoshimoto T, Harada N, Yada M, Kato M, Kotoh K, Taketomi A, Maehara Y, Nakashima M, Enjoji M.** 2010. Expression profile of lipid metabolism-associated genes in hepatitis C virus-infected human liver. *Hepatology* **40**:923-929.
16. **Lerat H, Kammoun HL, Hainault I, Merour E, Higgs MR, Callens C, Lemon SM, Foufelle F, Pawlotsky JM.** 2009. Hepatitis C virus proteins induce lipogenesis and defective triglyceride secretion in transgenic mice. *J Biol Chem* **284**:33466-33474.
17. **Li Q, Pene V, Krishnamurthy S, Cha H, Liang TJ.** 2013. Hepatitis C virus infection activates an innate pathway involving IKK-alpha in lipogenesis and viral assembly. *Nat Med* **19**:722-729.
18. **Leandro G, Mangia A, Hui J, Fabris P, Rubbia-Brandt L, Colloredo G, Adinolfi LE, Asselah T, Jonsson JR, Smedile A, Terrault N, Paziienza V, Giordani MT, Giostra E, Sonzogni A, Ruggiero G, Marcellin P, Powell EE, George J, Negro F, Group HCVM-AIPDS.** 2006. Relationship between steatosis, inflammation, and fibrosis in chronic hepatitis C: a meta-analysis of individual patient data. *Gastroenterology* **130**:1636-1642.
19. **Castera L, Chouteau P, Hezode C, Zafrani ES, Dhumeaux D, Pawlotsky JM.** 2005. Hepatitis C virus-induced hepatocellular steatosis. *Am J Gastroenterol* **100**:711-715.
20. **Bugianesi E, Salamone F, Negro F.** 2012. The interaction of metabolic factors with HCV infection: does it matter? *J Hepatol* **56 Suppl 1**:S56-65.
21. **Nourbakhsh M, Douglas DN, Pu CH, Lewis JT, Kawahara T, Lisboa LF, Wei E, Asthana S, Quiroga AD, Law LM, Chen C, Addison WR, Nelson R, Houghton M, Lehner R, Kneteman NM.** 2013. Arylacetamide deacetylase: a novel host factor with important roles in the lipolysis of cellular triacylglycerol stores, VLDL assembly and HCV production. *J Hepatol* **59**:336-343.
22. **Moriya K, Yotsuyanagi H, Shintani Y, Fujie H, Ishibashi K, Matsuura Y, Miyamura T, Koike K.** 1997. Hepatitis C virus core protein induces hepatic steatosis in transgenic mice. *J Gen Virol* **78 (Pt 7)**:1527-1531.
23. **Lerat H, Honda M, Beard MR, Loesch K, Sun J, Yang Y, Okuda M, Gosert R, Xiao SY, Weinman SA, Lemon SM.** 2002. Steatosis and liver cancer in transgenic mice expressing the structural and nonstructural proteins of hepatitis C virus. *Gastroenterology* **122**:352-365.
24. **Piodi A, Chouteau P, Lerat H, Hezode C, Pawlotsky JM.** 2008. Morphological changes in intracellular lipid droplets induced by different hepatitis C virus genotype core sequences and relationship with steatosis. *Hepatology* **48**:16-27.
25. **Harris C, Herker E, Farese RV, Jr., Ott M.** 2011. Hepatitis C virus core protein decreases lipid droplet turnover: a mechanism for core-induced steatosis. *J Biol Chem* **286**:42615-42625.
26. **Camus G, Schweiger M, Herker E, Harris C, Kondratowicz AS, Tsou CL, Farese RV, Jr., Herath K, Previs SF, Roddy TP, Pinto S, Zechner R, Ott M.** 2014. The Hepatitis C Virus Core Protein Inhibits Adipose Triglyceride Lipase (ATGL)-mediated Lipid Mobilization and Enhances the ATGL Interaction with Comparative Gene Identification 58 (CGI-58) and Lipid Droplets. *J Biol Chem* **289**:35770-35780.
27. **Inohara N, Koseki T, Chen S, Wu X, Nunez G.** 1998. CIDE, a novel family of cell death activators with homology to the 45 kDa subunit of the DNA fragmentation factor. *EMBO J* **17**:2526-2533.

- 551 28. **Wu X, Robotham JM, Lee E, Dalton S, Kneteman NM, Gilbert DM, Tang H.** 2012.
552 Productive hepatitis C virus infection of stem cell-derived hepatocytes reveals a critical
553 transition to viral permissiveness during differentiation. *PLoS Pathog* **8**:e1002617.
- 554 29. **Wu X, Lee EM, Hammack C, Robotham JM, Basu M, Lang J, Brinton MA, Tang H.**
555 2014. Cell death-inducing DFFA-like effector b is required for hepatitis C virus entry into
556 hepatocytes. *J Virol* **88**:8433-8444.
- 557 30. **Liu K, Zhou S, Kim JY, Tillison K, Majors D, Rearick D, Lee JH, Fernandez-**
558 **Boyanapalli RF, Barricklow K, Houston MS, Smas CM.** 2009. Functional analysis of
559 FSP27 protein regions for lipid droplet localization, caspase-dependent apoptosis, and
560 dimerization with CIDEA. *Am J Physiol Endocrinol Metab* **297**:E1395-1413.
- 561 31. **Erdtmann L, Franck N, Lerat H, Le Seyec J, Gilot D, Cannie I, Gripon P, Hibner U,**
562 **Guguen-Guillouzo C.** 2003. The hepatitis C virus NS2 protein is an inhibitor of CIDE-
563 B-induced apoptosis. *J Biol Chem* **278**:18256-18264.
- 564 32. **Zhou Z, Yon Toh S, Chen Z, Guo K, Ng CP, Ponniah S, Lin SC, Hong W, Li P.** 2003.
565 Cidea-deficient mice have lean phenotype and are resistant to obesity. *Nat Genet* **35**:49-
566 56.
- 567 33. **Nishino N, Tamori Y, Tateya S, Kawaguchi T, Shibakusa T, Mizunoya W, Inoue K,**
568 **Kitazawa R, Kitazawa S, Matsuki Y, Hiramatsu R, Masubuchi S, Omachi A,**
569 **Kimura K, Saito M, Amo T, Ohta S, Yamaguchi T, Osumi T, Cheng J, Fujimoto T,**
570 **Nakao H, Nakao K, Aiba A, Okamura H, Fushiki T, Kasuga M.** 2008. FSP27
571 contributes to efficient energy storage in murine white adipocytes by promoting the
572 formation of unilocular lipid droplets. *J Clin Invest* **118**:2808-2821.
- 573 34. **Ye J, Li JZ, Liu Y, Li X, Yang T, Ma X, Li Q, Yao Z, Li P.** 2009. Cideb, an ER- and
574 lipid droplet-associated protein, mediates VLDL lipidation and maturation by interacting
575 with apolipoprotein B. *Cell Metab* **9**:177-190.
- 576 35. **Tiwari S, Siddiqi S, Siddiqi SA.** 2013. CideB protein is required for the biogenesis of
577 very low density lipoprotein (VLDL) transport vesicle. *J Biol Chem* **288**:5157-5165.
- 578 36. **Li JZ, Lei Y, Wang Y, Zhang Y, Ye J, Xia X, Pan X, Li P.** 2010. Control of
579 cholesterol biosynthesis, uptake and storage in hepatocytes by Cideb. *Biochim Biophys*
580 *Acta* **1801**:577-586.
- 581 37. **Jiang J, Luo G.** 2012. Cell culture-adaptive mutations promote viral protein-protein
582 interactions and morphogenesis of infectious hepatitis C virus. *J Virol* **86**:8987-8997.
- 583 38. **Kaul A, Woerz I, Meuleman P, Leroux-Roels G, Bartenschlager R.** 2007. Cell culture
584 adaptation of hepatitis C virus and in vivo viability of an adapted variant. *J Virol*
585 **81**:13168-13179.
- 586 39. **Kim S, Date T, Yokokawa H, Kono T, Aizaki H, Maurel P, Gondeau C, Wakita T.**
587 2014. Development of hepatitis C virus genotype 3a cell culture system. *Hepatology*
588 **60**:1838-1850.
- 589 40. **Ding Y, Zhang S, Yang L, Na H, Zhang P, Zhang H, Wang Y, Chen Y, Yu J, Huo C,**
590 **Xu S, Garaiova M, Cong Y, Liu P.** 2013. Isolating lipid droplets from multiple species.
591 *Nat Protoc* **8**:43-51.
- 592 41. **Mercer DF, Schiller DE, Elliott JF, Douglas DN, Hao C, Rinfret A, Addison WR,**
593 **Fischer KP, Churchill TA, Lakey JR, Tyrrell DL, Kneteman NM.** 2001. Hepatitis C
594 virus replication in mice with chimeric human livers. *Nat Med* **7**:927-933.

42. **Singaravelu R, Lyn RK, Srinivasan P, Delcorde J, Steenbergen RH, Tyrrell DL, Pezacki JP.** 2013. Human serum activates CIDEB-mediated lipid droplet enlargement in hepatoma cells. *Biochem Biophys Res Commun* **441**:447-452.
43. **Eden E, Geva-Zatorsky N, Issaeva I, Cohen A, Dekel E, Danon T, Cohen L, Mayo A, Alon U.** 2011. Proteome half-life dynamics in living human cells. *Science* **331**:764-768.
44. **Franch HA, Sooparb S, Du J, Brown NS.** 2001. A mechanism regulating proteolysis of specific proteins during renal tubular cell growth. *J Biol Chem* **276**:19126-19131.
45. **Boulant S, Targett-Adams P, McLauchlan J.** 2007. Disrupting the association of hepatitis C virus core protein with lipid droplets correlates with a loss in production of infectious virus. *J Gen Virol* **88**:2204-2213.
46. **Chan SC, Lin SC, Li P.** 2007. Regulation of Cidea protein stability by the ubiquitin-mediated proteasomal degradation pathway. *Biochem J* **408**:259-266.
47. **Nian Z, Sun Z, Yu L, Toh SY, Sang J, Li P.** 2010. Fat-specific protein 27 undergoes ubiquitin-dependent degradation regulated by triacylglycerol synthesis and lipid droplet formation. *J Biol Chem* **285**:9604-9615.
48. **Singaravelu R, Delcorde J, Lyn RK, Steenbergen RH, Jones DM, Tyrrell DL, Russell RS, Pezacki JP.** 2014. Investigating the antiviral role of cell death-inducing DFF45-like effector B in HCV replication. *FEBS J* **281**:3751-3765.
49. **Vogt DA, Camus G, Herker E, Webster BR, Tsou CL, Greene WC, Yen TS, Ott M.** 2013. Lipid droplet-binding protein TIP47 regulates hepatitis C Virus RNA replication through interaction with the viral NS5A protein. *PLoS Pathog* **9**:e1003302.
50. **Boulant S, Douglas MW, Moody L, Budkowska A, Targett-Adams P, McLauchlan J.** 2008. Hepatitis C virus core protein induces lipid droplet redistribution in a microtubule- and Dynein-dependent manner. *Traffic* **9**:1268-1282.
51. **Foy E, Li K, Wang C, Sumpter R, Jr., Ikeda M, Lemon SM, Gale M, Jr.** 2003. Regulation of interferon regulatory factor-3 by the hepatitis C virus serine protease. *Science* **300**:1145-1148.
52. **Li XD, Sun L, Seth RB, Pineda G, Chen ZJ.** 2005. Hepatitis C virus protease NS3/4A cleaves mitochondrial antiviral signaling protein off the mitochondria to evade innate immunity. *Proc Natl Acad Sci U S A* **102**:17717-17722.

Figure Legends

Fig. 1. HCV infection downregulates CIDEB in vitro and in vivo. (A)

Immunofluorescence staining of viral proteins and CIDEB. Huh-7.5-based CIDEB-KO cells (clone #3) stably expressing FLAG-CIDEB were infected with a high-titer JFH-1 (HCV) variant, JFH-1/AD16 (genotype 2), for 3 days before co-staining for FLAG and HCV NS3. FLAG-CIDEB CBKO#3 cells were infected with VSV-GFP for 16 hours, stained for FLAG-CIDEB, and analyzed for co-expression of FLAG-CIDEB and GFP. FLAG-CIDEB CBKO#3 cells were infected with DENV for 48 hours, and co-stained for FLAG-CIDEB and DENV NS3. (B) Immunoblot of CIDEB in genotype 2 (top panels) or genotype 3 (bottom panels)-infected cells. Cells were infected for 3 days with various genotype 2a virus before analysis by western blot or for 8 days with various genotype 3a-based (S310) clones or the S310/JFH-1 chimera. On day 8 post-infection, core protein was measured from the supernatants by HCV core-specific ELISA, and cell lysates were analyzed by western blot for CIDEB. Beta-actin was included as a loading control. (C) CIDEB protein levels in HCV-infected uPA/SCID humanized mouse model. Liver tissue lysates from primary human hepatocytes (PHH)-transplanted uPA/SCID mice, either uninfected (n=5) or HCV infected (n=5), were subjected to western blot to measure CIDEB protein levels. Data from individual mice are plotted as CIDEB protein normalized to GAPDH protein (control). Quantification of band intensity was performed using the ImageJ software (National Institutes of Health). HCV-infected versus non-infected humanized mice showed statistically significant levels of CIDEB protein ($p = 0.01$). Measured HCV titers (in RNA copies/mL) are listed in the adjacent table.

Fig. 2. Endogenous CIDEB is a short-lived protein that is post-translationally regulated via the ubiquitin-proteasome pathway. (A) Cells were treated with the protein synthesis inhibitor CHX for 0, 1, 2, or 3 hours, then lysed and analyzed by western blot for CIDEB protein levels. GAPDH was included as a loading control. (B) Treatment with the proteasome inhibitor MG132 blocked CIDEB degradation in both wildtype cells and in cells harboring a lentivirus encoding shRNA targeting CIDEB mRNA. (C) Analysis of CIDEB ubiquitination. Cells were co-transfected with FLAG-CIDEB or a FLAG-control protein (Prp31c) and HA-ubiquitin constructs, followed by MG132 treatment, co-immunoprecipitation with anti-FLAG beads, and western blot. (D) A schematic of FLAG-CIDEB deletion constructs used for stability analysis. (E) Stability of CIDEB deletion mutants. Cells were transfected with various FLAG-CIDEB-encoding constructs (represented in D) and subsequently treated with CHX, 24 hours post transfection, for 4 hours, before immunoblot analysis using FLAG-specific antibody. (F) The point mutation K173A enhanced CIDEB stability. Cells transfected with wildtype or K173A CIDEB mutant cDNA were treated with CHX, collected at the indicated times, and analyzed similar to (A).

Fig. 3. HCV-infected cells exhibit lower levels of CIDEB protein, likely through a proteolytic cleavage event. (A) Effect of HCV infection on endogenous CIDEB protein. Western blot analysis of Huh-7.5 cells infected with JFH-1/AD16 for 3 days revealed a faster-migrating band recognized by the CIDEB antibody, in addition to the full-length product. The asterisk indicates a degradation product occasionally seen from uninfected Huh-7.5 cells. (B) Effect of proteasome inhibition on CIDEB protein levels in HCV

674 infected cells. Huh-7.5 cells were infected with JFH-1/AD16 for 48 hours, then treated
675 with MG132 for 18 hours before analysis by western blot. A longer exposure of GAPDH,
676 CIDEB and the CIDEB cleavage product are shown to the right. (C) Effect of HCV
677 infection on N-terminally FLAG-tagged CIDEB. Western blot analysis of CIDEB-KO cells
678 (clone #3) stably expressing FLAG-CIDEB and electroporated with JFH-1 for 3 days.
679 FLAG-CIDEB was detected by anti-CIDEB antibody. (D) Western blot analysis of
680 endogenous CIDEB and NS3 levels in Huh-7.5 cells with various HCV RNAs. Cells
681 were electroporated with 10 μ g of RNA generated from either wildtype or mutant
682 genomes and then analyzed 48 hours later for their ability to downregulate CIDEB.
683 Δ core: a Jc1/GLuc variant lacking the intact HCV capsid protein; GNN: a Jc1/GLuc
684 variant harboring a replication-deficient replicase. (E) Similar analysis of endogenous
685 CIDEB and NS3 levels in Huh-7.5 cells 48 hours after cells were electroporated with
686 10 μ g of RNA generated from either wildtype JFH-1 or Δ E1/E2-JFH-1, a viral-encoding
687 construct lacking the two HCV envelope proteins.

688

689 Fig. 4. Intracellular lipid abundance affects CIDEB protein stability. (A) Effect of two
690 structurally distinct lipid droplet inhibitors, PF-429242, a reversible inhibitor of
691 cholesterol synthesis and Triacsin C, an inhibitor of long-chain fatty acid acyl-CoA
692 synthetase, on LDs in Huh-7.5 cells. Cells were treated with 40 μ M PF-429242 or 5.5 μ M
693 of TriC for 24 hours before staining with ORO. (B) Cell viability was measured after 24
694 hours treatment with the indicated compound. (C and D) Western blot analysis of
695 CIDEB protein levels in Huh-7.5 cells treated with PF-429242 or TriC for 24 hours.
696 Quantification of CIDEB protein levels on western blot by ImageJ analysis (analyzed

from biological triplicates). Ku80 was used as a loading control. (E) 24 hour treatment of Huh-7.5 cells with PF-429242 or TriC do not significantly alter CIDEB mRNA levels. (F and G) Effect of exogenous lipid loading on CIDEB protein in infected cells. Uninfected or (24 hour) JFH-1/AD16 infected Huh-7.5 cells were treated with 100 μ M OA for 20 hours before being fixed for ORO staining or lysed for western blot analysis.

Fig. 5. (A) Effect of a JFH-1 core mutant deficient in LD-targeting on CIDEB cleavage. Western blot analysis of Huh-7.5 cells was performed 48 hours after electroporation of cells with 10 μ g of JFH-1 or JFH-DP RNA. (B) Localization of endogenous CIDEB and HCV core after HCV infection assayed by LD fractionation. 15 μ g of whole cell lysate (WCL) and 7.5 μ g of purified LD-associated proteins were analyzed by WB. (C) Co-localization of exogenously overexpressed FLAG-tagged CIDEB and HCV core protein on lipid droplets.

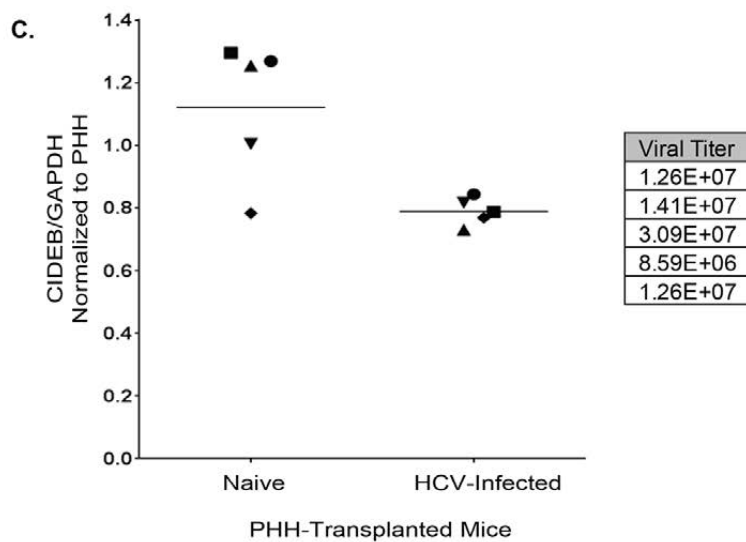
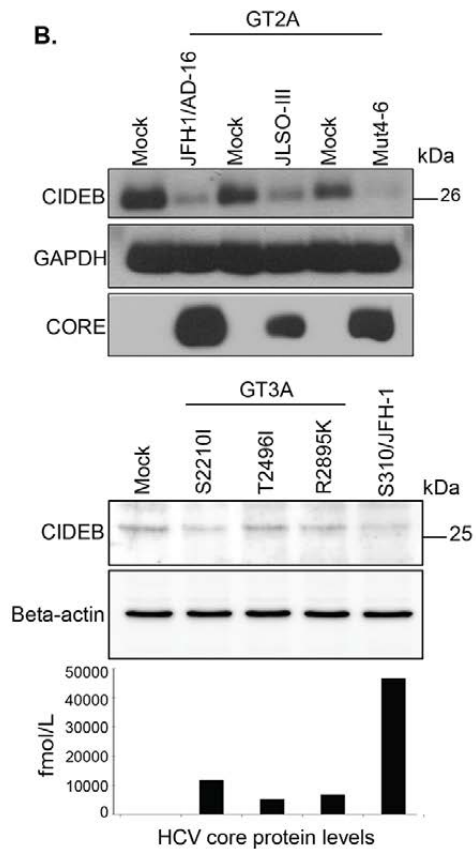
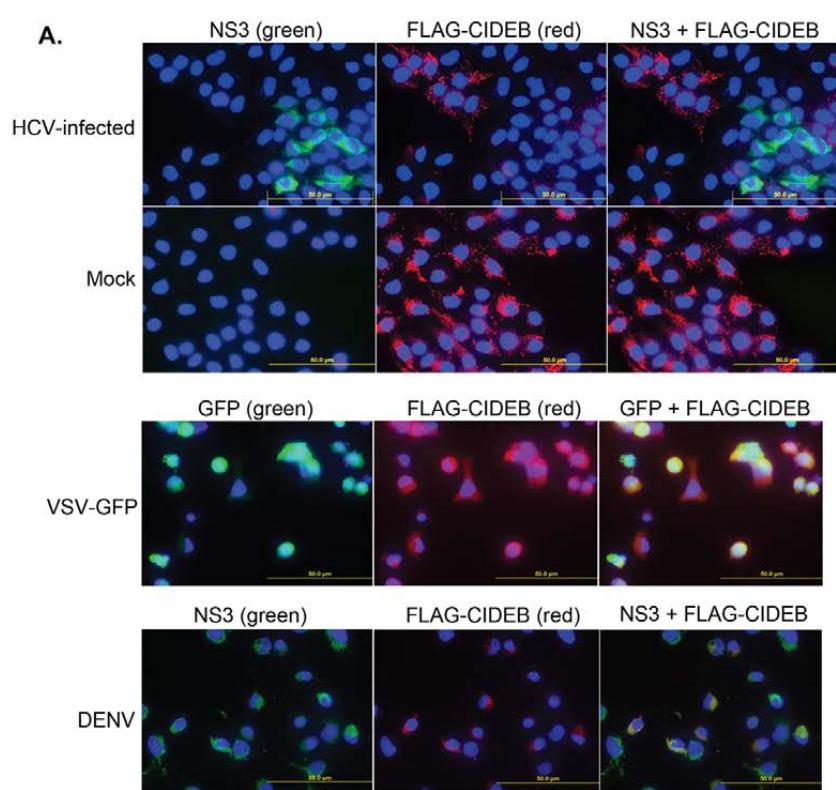
Fig. 6. CIDEB modulates LD stability. (A) LD stability in naïve or JFH-1/AD16 infected Huh-7.5 cells. Cells were incubated in lipid-rich medium for 14 hours, washed with PBS and cultured in DMEM with 5.5 μ M TriC for 24 hours before staining with ORO (red, 100x) and DAPI (blue), or anti-NS3 (green, 40x) and DAPI. (B) Formation of LDs in Huh-7.5 or Huh-7.5 CIDEB-KO after lipid loading. Cells were incubated in the lipid-rich medium for 20 hours, washed with PBS and stained for LDs using ORO (red, 100x). (C) LD stability in wildtype and CIDEB KO cells. After lipid loading as above, cells were cultured in DMEM with or without 5.5 μ M of TriC for 24 hours and then stained for LDs

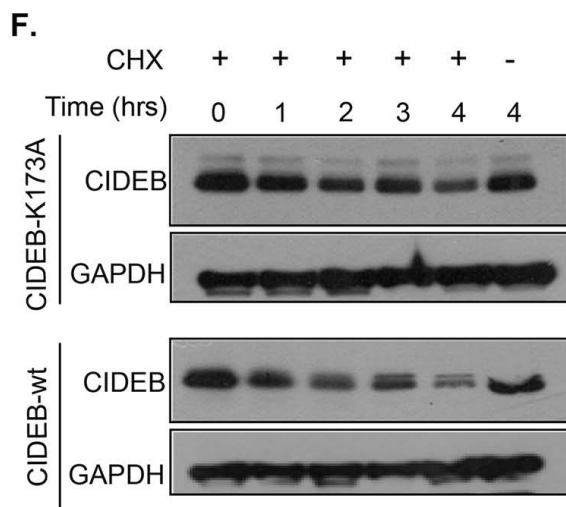
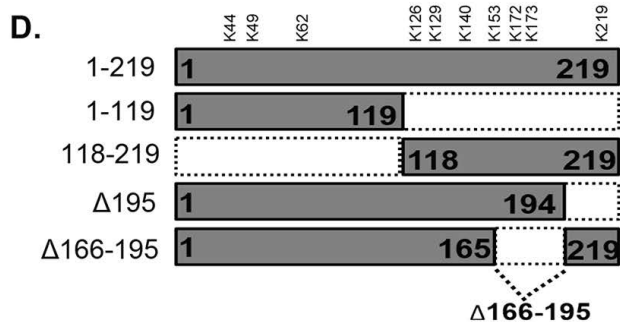
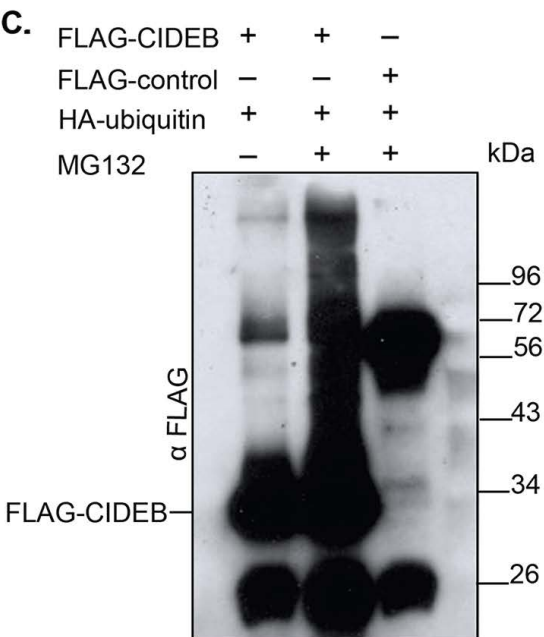
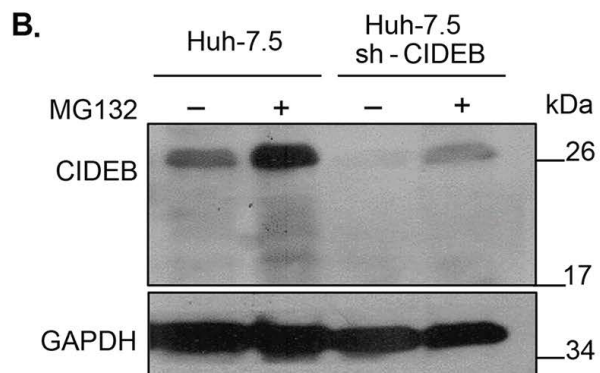
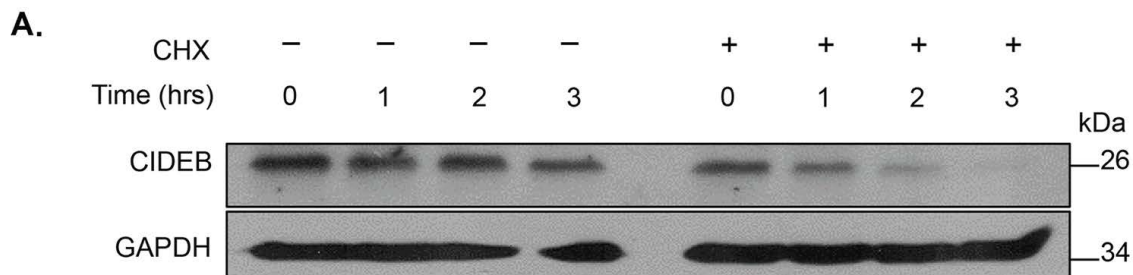
using ORO (red, 100x). Panels 1, 2, and 3 are separate frames. DAPI (blue) was used as a counterstain.

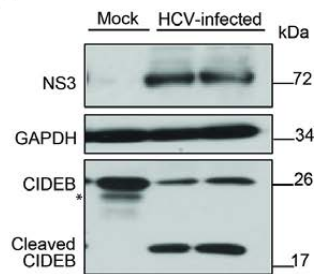
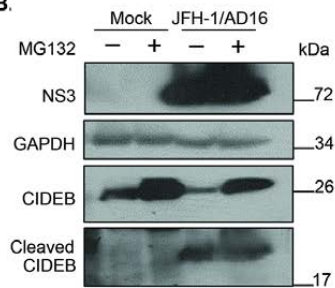
Fig. 7. Knockout of CIDEA in human hepatoma cells results in altered VLDL secretion and TG storage. (A) Secreted and intracellular TG in Huh-7.5 or Huh-7.5 CIDEA-KO (clone #11) cells. Cells were cultured in a lipid-rich medium (supplemented with 375 μ M OA) for 20 hours, washed with PBS and then either collected for lysate or further incubated in fresh DMEM for 2 hours for supernatant collection. Both lysate and supernatant were analyzed for TG contents. (B) Analysis of secreted and intracellular ApoB levels. Huh-7.5 cells or Huh-7.5 CIDEA-KO (clone #11) cells were cultured in a lipid-rich medium (supplemented with 375 μ M OA) for 14 hours, washed with PBS and then further incubated in fresh DMEM for 8 hours for supernatant collection. (C) Lipid density profile of secreted ApoB-associated VLDL particles. Fractions of the supernatant collected above were analyzed for amount of ApoB protein in each fraction. Distribution of ApoB-containing particles of different densities are quantified and plotted. Data from three replicate experiments are shown. (D) Lipid density profile of secreted ApoB-associated VLDL particles in HCV infected cells. Naïve and 60 hour post-JFH-1/AD16 infected Huh-7.5 cells were cultured in a lipid-rich medium (supplemented with 375 μ M OA) for 14 hours, washed with PBS and then further incubated in fresh DMEM for 8 hours for supernatant collection. Fractions of the supernatant collected above were analyzed for amount of ApoB protein in each fraction. Distribution of ApoB-containing particles of different densities are quantified and plotted. Data from two biological replicate experiments are shown.

743 Fig. 8. Potential mechanism for HCV-mediated CIDEB downregulation. CIDEB protein
744 levels are normally regulated by the ubiquitin-proteasome pathway (A). In the infected
745 cells, HCV core is trafficked onto LDs (B), which may result in competitive displacement
746 of CIDEB off the LD surface (C), exposing CIDEB to a protease. Reduced level of
747 CIDEB results in altered VLDL lipid profile (D), through a mechanism involving the
748 reported CIDEB – ApoB interaction (E) (34).

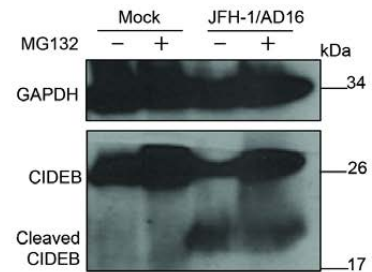
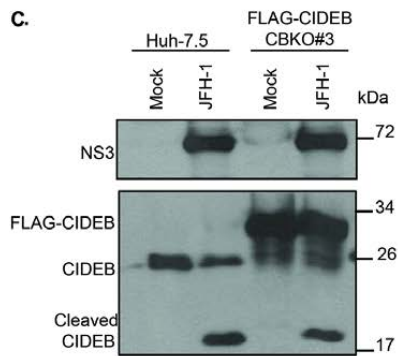
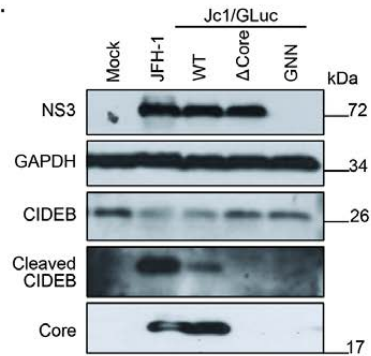
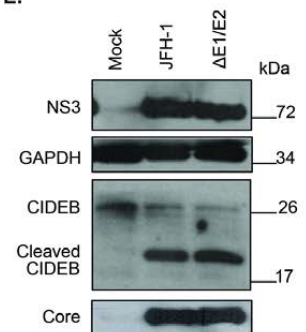
749

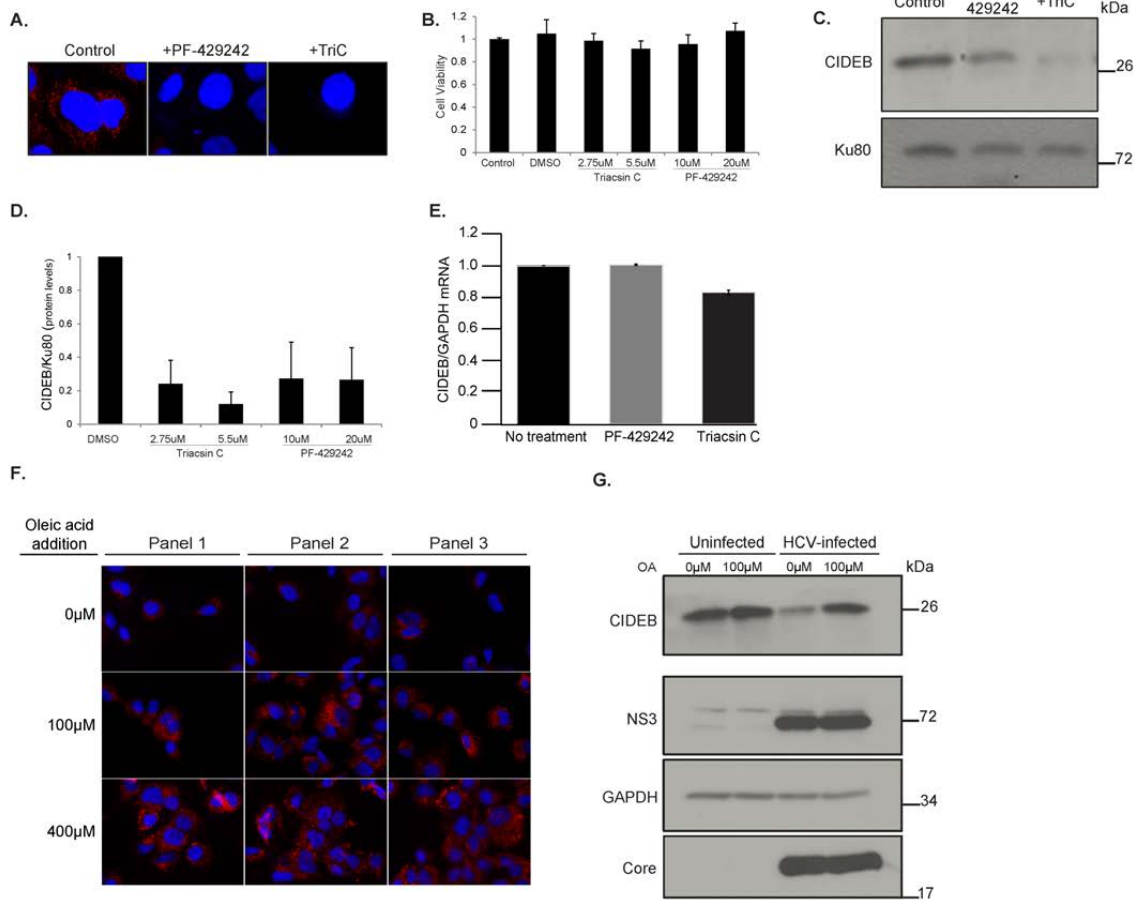


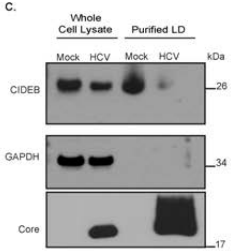
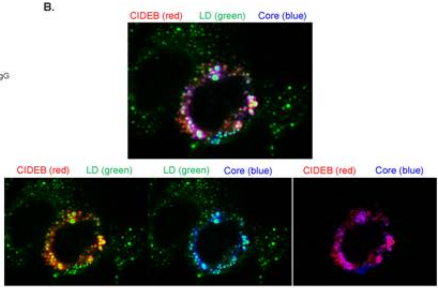
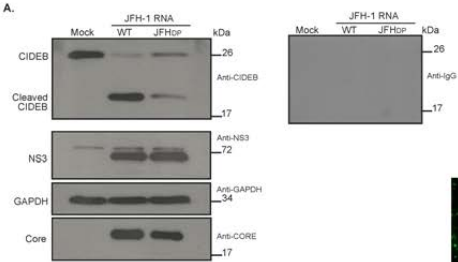


A.**B.**

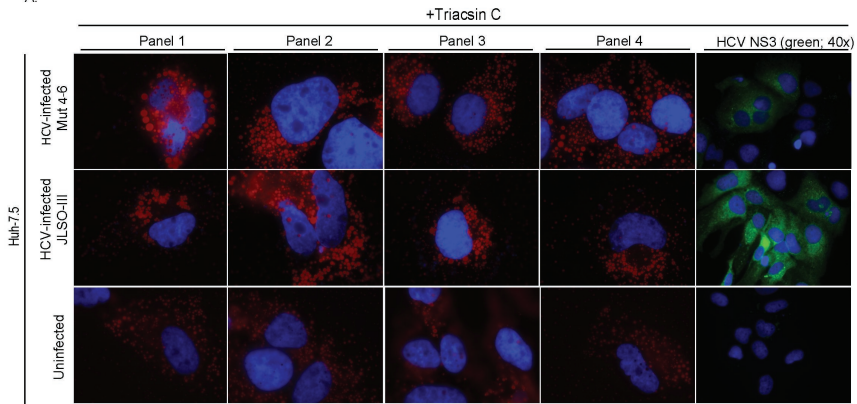
(Longer Exposure)

**C.****D.****E.**





A.



B.

